**Stanisław Rabiej,
Włodzimierz Biniaś,
Dorota Biniaś**

Akademia Techniczno Humanistyczna
ul. Willowa, 243-309 Bielsko-Biała

The Transition Phase in Polyethylenes – WAXS and Raman Investigations

Abstract
The existence of the third, transition component, apart from the crystalline and amorphous phases, in polyethylenes has already been proved in several papers. In this work, the WAXS patterns of polyethylenes with various branch contents were analysed, aiming at the best method of accounting for the third phase in the procedure of decomposition of the patterns into crystalline peaks and amorphous scattering. It appeared that the best result was obtained when we assumed that the intermediate phase is represented by two peaks located close to the crystalline reflections (110) and (200), on the left sides of these reflections. The calculations performed have shown that both the density and the mass fraction of this intermediate third phase decrease continuously with increasing 1-octene content. A comparison of the mass fractions of the three phases has shown that the total mass fractions of the crystalline and transition phases determined with the WAXS and Raman methods coincide very well; however, the values obtained for each individual phase do not agree with one another.

Key words: *WAXS, Raman spectroscopy, transition phase, crystallinity, polyethylene.*

Introduction

The analysis of Wide Angle X-ray Scattering (WAXS) curves for various polyethylenes (this name covers polyethylene and ethylene-1-alkene copolymers of different degrees of branching) leads to the conclusion that the proper description of their structure needs the introduction of a transition phase – an intermediate component in addition to the crystalline and amorphous phases. Such a conclusion has already been presented in several papers [1-4]. It was shown [4], that for a polyethylene in a solid state, both the angular position 2θ of the amorphous halo as well as its width at half height are considerably higher than the values expected from the extrapolation of the respective data for this polymer in a molten state. This fact suggests that the amorphous halo of a polyethylene in a solid state is a sum of scattering from a completely amorphous, liquid-like phase and from the intermediate, better-ordered regions that originate during crystallization. So, in analysing the WAXS profiles, we have to determine how to account for this third component in the deconvolution of the diffractogram.

In this work, a series of ethylene-1-octene homogeneous copolymers with a 1-octene content ranging from 0.8 to 11.27 mol% and a linear polyethylene standard were investigated. In contrast to other similar investigations, the WAXS patterns were analysed in a broad 2θ range: 4°–60°, covering not only the highest (200) and (110) peaks but all the peaks characteristic of the crystalline phase, located at higher 2θ angles. The mass fractions of all three phases were calculated with the WAXS method and compared with those obtained from the analysis of the Raman spectra of the investigated polymers, which was performed using the method developed by Strobl and Hagedorn [5].

Experimental

Material

The measurements were carried out for 8 homogeneous ethylene-1-octene copolymers synthesized at DSM Research (the Netherlands) using a metalocene catalyst system. The number of CH_3 groups per 1000 carbon atoms in the main chain (CH_3/1000 – degree of branching) and mole % of 1-octene provided by the producer are given in ***Table 1***. The melting temperatures were determined by independent DSC measurements. Additionally, the samples of linear polyethylene (LPE) and a commercial high-density polyethylene (HDPE) were investigated as the reference samples. Before the measurements, all the samples were melted at a temperature higher than their respective melting temperatures to erase their thermal history and cooled at the same rate of 10 °C/min to room temperature. The crystallinity of the samples was determined using the wide-angle X-ray diffraction (WAXS) and Raman spectroscopic methods.

WAXS method

Diffraction patterns were recorded in a symmetrical reflection mode using a URD-6 Seifert diffractometer and a copper target X-ray tube (λ = 1.54 Å) operated at 40 kV and 30 mA. Cu Kα radiation was monochromized with a graphite monochromizer. WAXS curves were recorded in the 2θ range 4°-60°, with a step of 0.1°. The samples had the shape of circular plates with a radius of 1 cm and a thickness of 1 mm.

Raman spectroscopic method

The Raman spectra of the investigated samples were recorded in the range of 3700-100 cm^{-1} with a resolution of 4 cm^{-1}, using the MICROSTAGE adapter of the Raman module of the Magna–IR 860 FTIR spectrometer (Nicolet) equipped with a YAG laser. The wavelength was 1064 nm, the diameter of the beam was 50 μm and its power 0.6 W. Each spectrum was obtained as the average of 2000 scans.

Results and discussion

The analysis and decomposition of the WAXS curves into component peaks and all the calculations were performed using WAXSFIT [6], a new version of

Table1. *Samples characteristics. CH_3/1000 is a number of CH_3 groups per 1000 atoms in the main chain of a copolymer.*

Sample	LPE	EO1	EO2	EO3	EO4	EO5	EO6	EO7	EO8
CH_3/1000	0	3.9	8.4	19.2	23.3	23.6	27.7	35.9	42.1
Mole % of 1-octene	0	0.8	1.77	4.34	5.42	5.5	6.64	9.15	11.27
Melting Temperature [°C]	132	130	119	101	96.3	94.1	92.3	69.5	60.5

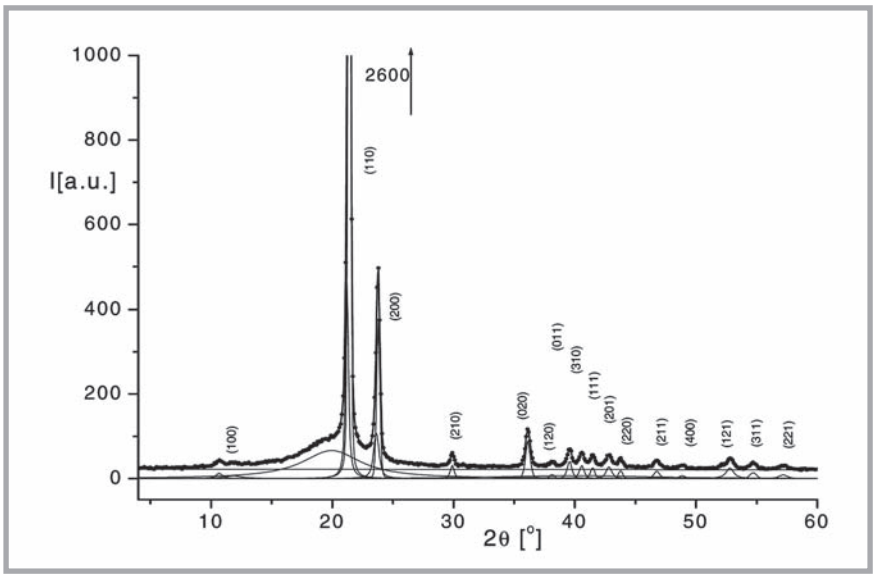

Figure 1. *WAXS pattern of linear polyethylene standard resolved into crystalline peaks and amorphous scattering.*

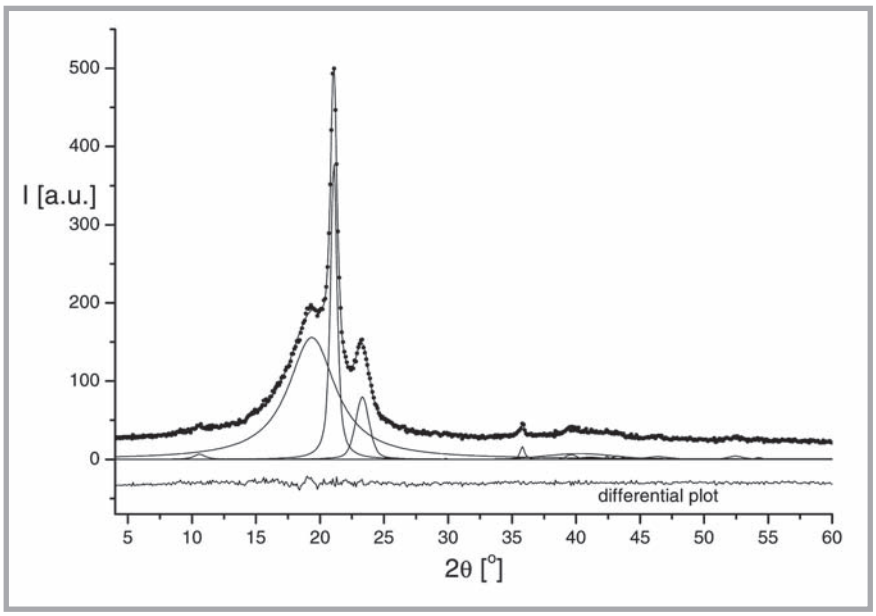

Figure 2. *WAXS pattern of the EO6 sample resolved into crystalline peaks and amorphous scattering, assuming a two-phase structure.*

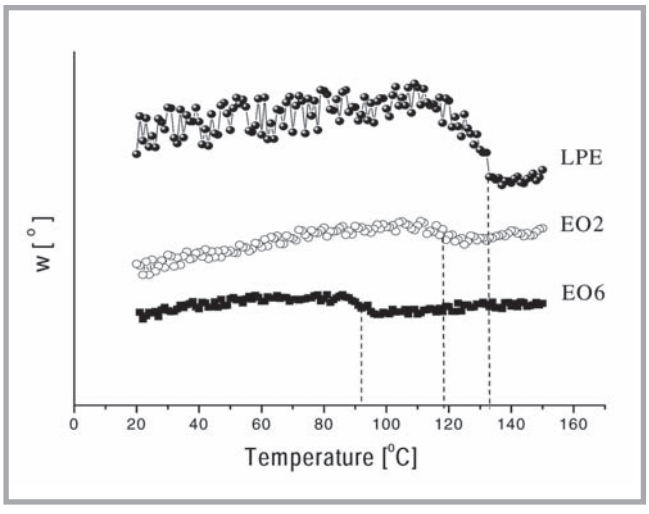

Figure 3. *Width at half height of the first amorphous maximum during cooling for LPE and two chosen copolymers EO2 and EO7 [4]. The dotted lines indicate the melting temperatures.*

the Optifit [7] computer program. In the first stage, a linear background was determined based on the intensity level at small and large angles and subtracted from the diffraction curves. Next, the curves of all the samples were normalized to the same value of integral intensity scattered by a sample over the whole range of scattering angles recorded in the experiment. Finally, the diffraction curves were resolved into crystalline peaks and amorphous scattering. To this aim, a theoretical curve was constructed, composed of functions related to individual crystalline peaks and amorphous halos. The theoretical curve was fitted to the experimental one using a multicriterial optimization procedure and a hybrid system [8] that combines a genetic algorithm and the classical optimization method of Powell. Both crystalline peaks and amorphous halos were represented by a linear combination of Gauss and Lorentz profiles:

$$F_i(x) = f_i H_i \exp\left\{-\ln 2\left[\frac{2(x-x_{oi})}{w_i}\right]^2\right\} + \frac{(1-f_i)H_i}{1+[2(x-x_{oi})/w_i]^2} \quad (1)$$

where:
x – scattering angle 2θ, H_i – peak height, w_i – width at half height, x_{oi} – peak position, f_i – shape factor, f_i equals 0 for Lorentz profile and 1 for Gauss profile.

The starting values of the crystalline peak positions were calculated using the polyethylene unit cell dimensions. In contrast to other similar investigations, the WAXS patterns were recorded and analysed in a broad 2θ range: 4°–60° covering not only the highest (200) and (110) peaks but all the peaks characteristic of the crystalline phase, located at higher 2θ angles. The amorphous scattering was approximated by two broad maxima. The first maximum, located at lower diffraction angles, results from the inter-molecular scattering and the second one observed at higher angles results from intra-molecular scattering [9, 10]. In the case of polyethylenes, the maxima are located at $2\theta \approx$ 19–20° and $2\theta \approx$ 39–40°. The diffraction curve of LPE resolved into components is shown in ***Figure 1***.

In the first trials, the diffraction curves were resolved into components assuming an ideal two-phase structure of the investigated polymers. In the 2θ range, 10°–30°, the experimental curve was approximated by two

peaks representing (200) and (110) crystalline reflections and a broad peak representing the first amorphous maximum. However, for all the samples, the quality of fit was poor. An example is given in ***Figure 2***, which is related to the sample EO6. The differential plot shows considerable differences between the experimental and theoretical curves in the 2θ range corresponding to the considered peaks.

These problems with fitting are consistent with the results of our previous studies [4], which have indicated a composed structure of the amorphous scattering in the WAXS patterns of LPE and ethylene-1-octene copolymers. It was shown that the position, the width at half height and the shape of the first amorphous maximum change with the temperature of a polymer and the most sudden changes occur during melting or crystallization. In a solid state, the value of the angular position 2θ of the amorphous maximum as well as its width at half height are considerably higher than the values expected from the extrapolation of the respective data for molten polymer (***Figure 3*** [4]).

The abruptly changing width and the sudden change in the shape of the amorphous maximum, as well as the shift in its position, suggest that the amorphous phase contains two contributions and the total amorphous scattering is composed of two parts. One part is related to a typical liquid-like amorphous phase and the other one to better-ordered and denser regions. The changes observed during cooling and heating can be interpreted as being caused by the originating and disappearing of those partially ordered regions.

Based on these results, we assumed a 3-phase structure of the investigated polymers and tried to account for the third phase in the deconvolution of the diffractogram. At the beginning, we employed a 4-peak approximation in the 2θ range 12°–30°: 2 crystalline reflections (110) and (200), the amorphous maximum and the fourth peak were related to the intermediate phase. Such an approach is equivalent to the assumption of a quasi-hexagonal structure of the third phase. Unfortunately, the quality of fitting did not increase satisfactorily – the differential plot still showed clearly visible errors in the fitting of the curves. A plot obtained for the sample EO6 is given in ***Figure 4***. For this reason, we adopted the ideas of Baker and Windle[11] in our further analysis. Investigating several polyethylenes with a broad range of branching, Baker noticed that the unit cell parameters refined from the fitting of the theoretical curve just to the (110) and (200) reflections were clearly larger than those refined from the higher angle reflections. The extent of the discrepancy was higher, the more branched the polyethylenes were. Baker has found that such an effect is caused by a clear asymmetry of the peaks (110) and (200). He indicated the excess scattering on the left, low-angle side of these peaks. Baker proposed that the excess scattering is produced by a third, partially ordered component of the polymer structure. Based on the difference plot between the theoretical and experimental curves, he showed that the scattering produced by the third component contains two peaks, which are broader, clearly smaller and shifted towards lower angles with respect to the "true" crystalline (110) and (200) reflections. Because of a lower degree of order, the contribution of the third phase to the weaker, higher angle crystalline reflections is negligible [11].

Adopting the suggestions of Baker, we decomposed the WAXS patterns, introducing two additional peaks related to the partially ordered component. This time, the quality

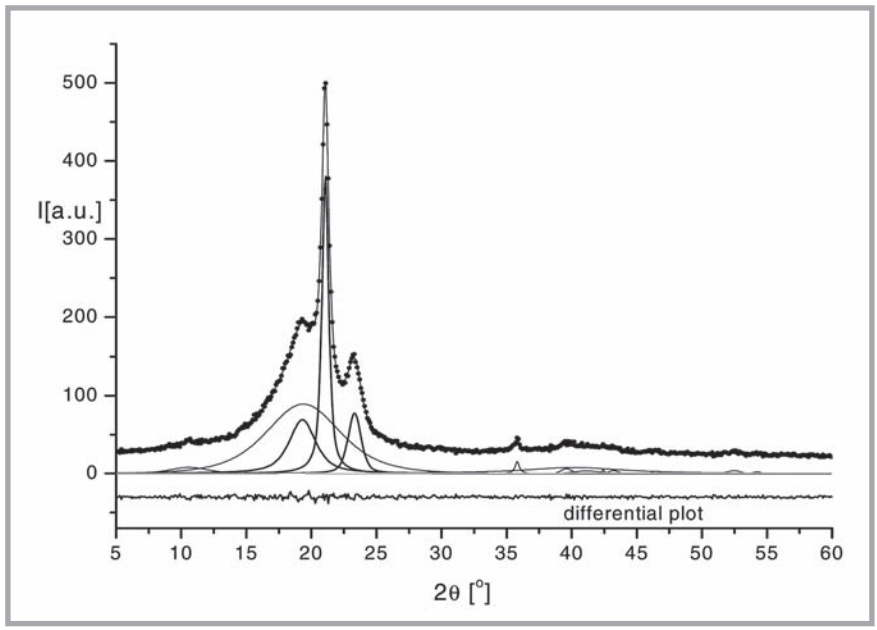

Figure 4. *WAXS pattern of the EO6 sample resolved into components. One additional peak represents a partially ordered phase.*

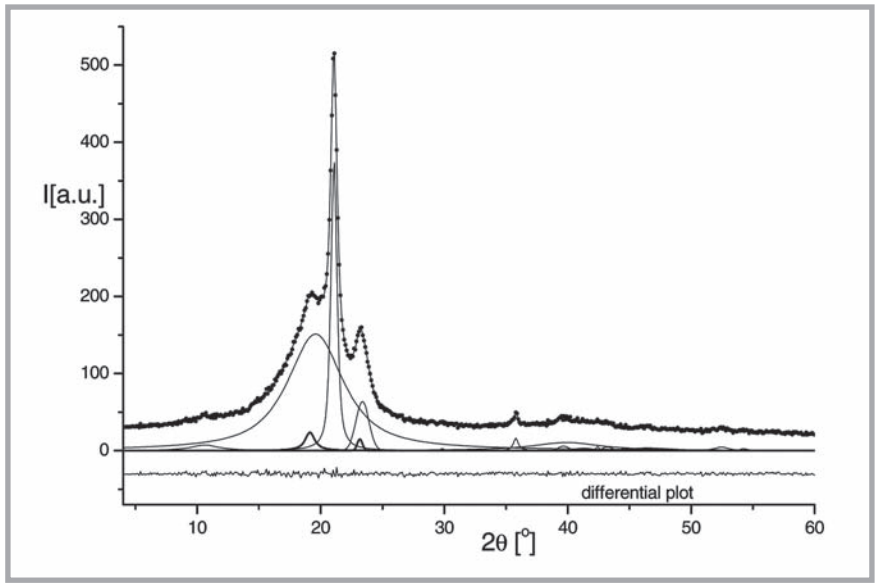

Figure 5. *WAXS pattern of the EO6 sample resolved into components. Two additional peaks represent a partially ordered phase.*

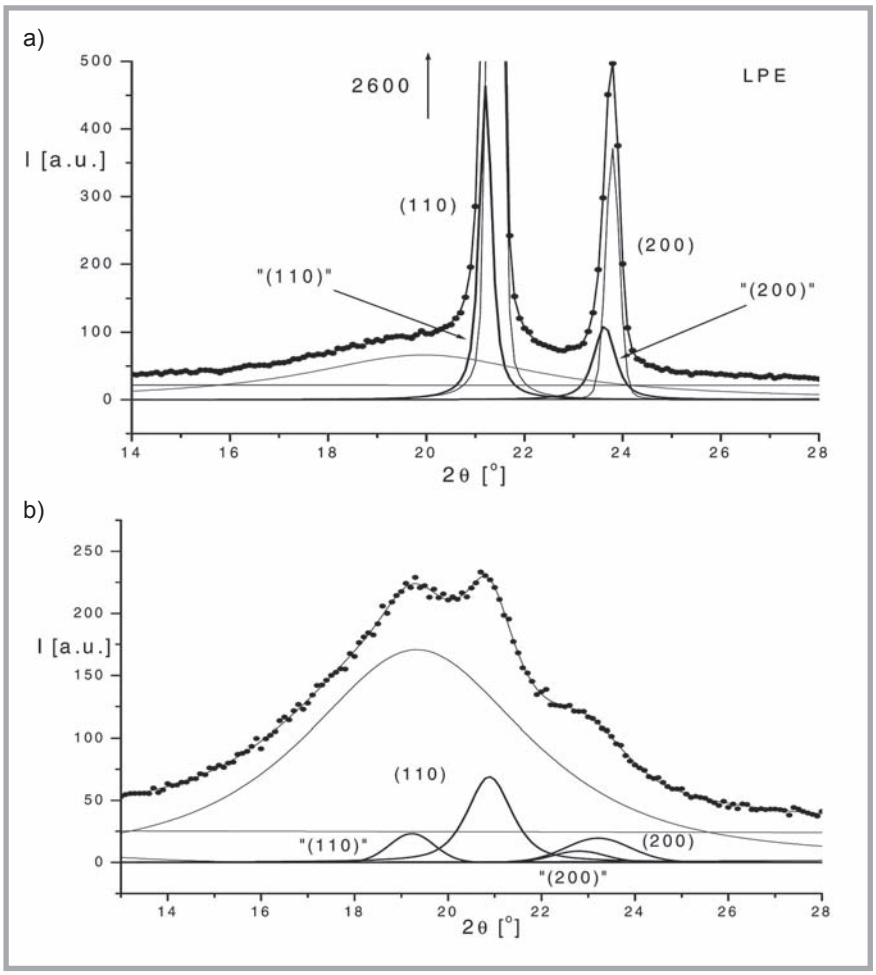

Figure 6. *WAXS pattern of the EO7 and LPE sample resolved into components. The peaks related to the transition phase are denoted as "(110)" and "(200)"; a) LPE sample, b) E07 sample.*

of fit was much better. The result of decomposition for the sample EO6 is shown in ***Figure 5*** (see page 59). In ***Figures 6.a*** and ***6.b***, similar plots but in a narrower angular range are shown for the samples LPE and EO7. Two additional peaks related to the transition phase are denoted by quotation marks: "(110)" and "(200)". It is seen that their shift with respect to the crystalline reflections (110) and (200) is much higher for the samples with high 1-octene content than for LPE. This means that the higher the degree of branching of a copolymer, the more loosely packed are the molecular chains in the transition regions. The calculated positions of the "(110)" and "(200)" peaks versus the number of CH_3 groups per 1000 carbon atoms in the main chain are shown in ***Figure 7***. Based on these angular positions and assuming a "quasi-orthorhombic" structure of the transition component, the *a* and *b* unit cell parameters and the density of this phase were estimated. In this estimation, it was assumed that the height of the unit cell (*c* edge) is the same as in crystalline polyethylene. The obtained results are shown in ***Figure 8***.

The density of the transition phase continuously decreases. In the case of LPE, it is close to the density of the crystalline phase of PE at room temperature (25 °C): 0.999 g/cm^3 [12]. For the sample with high 1-octene content, the density tends to the values typical of the amorphous phase: 0.851 g/cm^3 [12]. As can be seen in ***Figure 8***, the values obtained for the last two samples (EO7 and EO8) were estimated below this level. These errors are caused by the fact that the crystalline peaks in the WAXS patterns of these samples are broad and weak (see ***Figure 6.b***). As a consequence, the deconvolution of these patterns into component peaks may cause an incorrect estimation of their angular positions. Nevertheless, the trend in the observed changes in the density of the transition phase is clear and understandable. Most probably, the transition phase is located on the border between the crystalline and amorphous phases. It is formed of stretched sectors of molecular chains emerging from the surfaces of crystallites and partially retaining the alignment and order typical of the crystalline phase. In the case of linear polyethylene, the degree of packing of the chains in the transition regions, and consequently its density, is not too much less than in the crystallites. However, in the samples with a high concentration of branches formed of the 1-octene comonomer, the chains

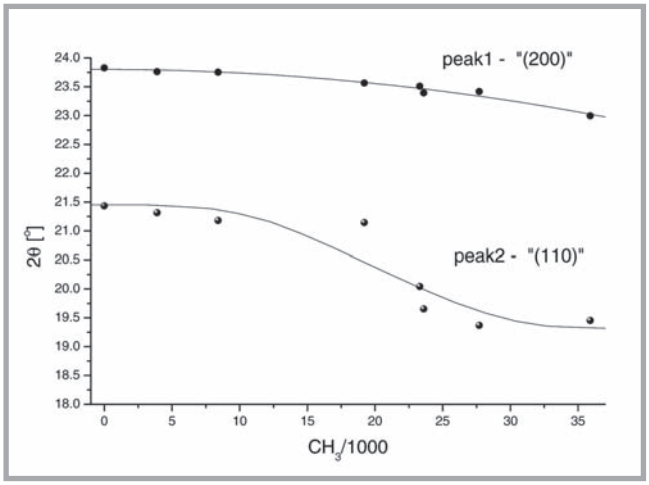

Figure 7. *Angular positions of the "(110)" and "(200)" peaks versus the number of CH_3/1000, calculated for all the investigated samples.*

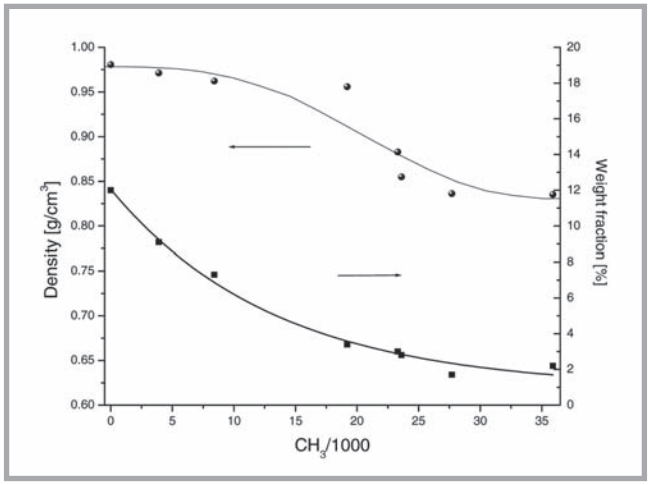

Figure 8. *Density and weight fraction of the third transition phase versus the number of CH_3/1000.*

emerging from the crystallites lose their alignment and order at much smaller distances from the surfaces of the crystallites and consequently the density of the transition regions tends to the density of the amorphous phase.

The mass fraction of the transition phase (T_X) was calculated as the ratio of the total area of the "(110)" and "(200)" peaks to the total area of the WAXS pattern after the background subtraction. In the same way, the mass fractions of crystalline (C_X) and amorphous (A_X) phases were calculated. The results of the calculations are given in ***Table 2*** (see page 62). As one can see, the mass fraction of the transition phase continuously decreases when the degree of branching increases. This result is fully consistent with that obtained in our first paper, resulting from the measurements of the angular position of the first amorphous maximum [4].

The mass fractions of all three phases were also determined using the method of Strobl and Hagedorn [5], which is based on the analysis of Raman spectra. In this method, the Raman spectra of the investigated samples are resolved into three components originating from the orthorhombic crystalline phase, a liquid-like amorphous phase and a third, partially ordered phase. According to Strobl and Hagedorn [5], the third phase is of a disordered, anisotropic structure, where the chains are stretched but have lost their lateral order. The mass fractions of these three phases are calculated directly from the integral intensities of characteristic bands.

The total, integral intensity of the CH_2 twisting vibrations range (1250-1350 cm^{-1}) is independent of the degree of crystallinity and for this reason can be used as a standard with which the intensities of other bands can be compared [5]. This range contains a narrow band localized at 1295 cm^{-1} arising from the crystalline phase and a much broader band at 1303 cm^{-1} coming from the liquid-like amorphous phase. The narrow band at 1416 cm^{-1} is a part of the CH_2 bending range, which is split into two component branches at 1416 cm^{-1} and 1440 cm^{-1} by the crystal field. For this reason, the band is related to the orthorhombic crystalline phase.

The mass fractions of the crystalline (C_R), liquid-like amorphous (A_R) and transition (T_R) phases contained in the investigated samples were calculated using the following formulas:

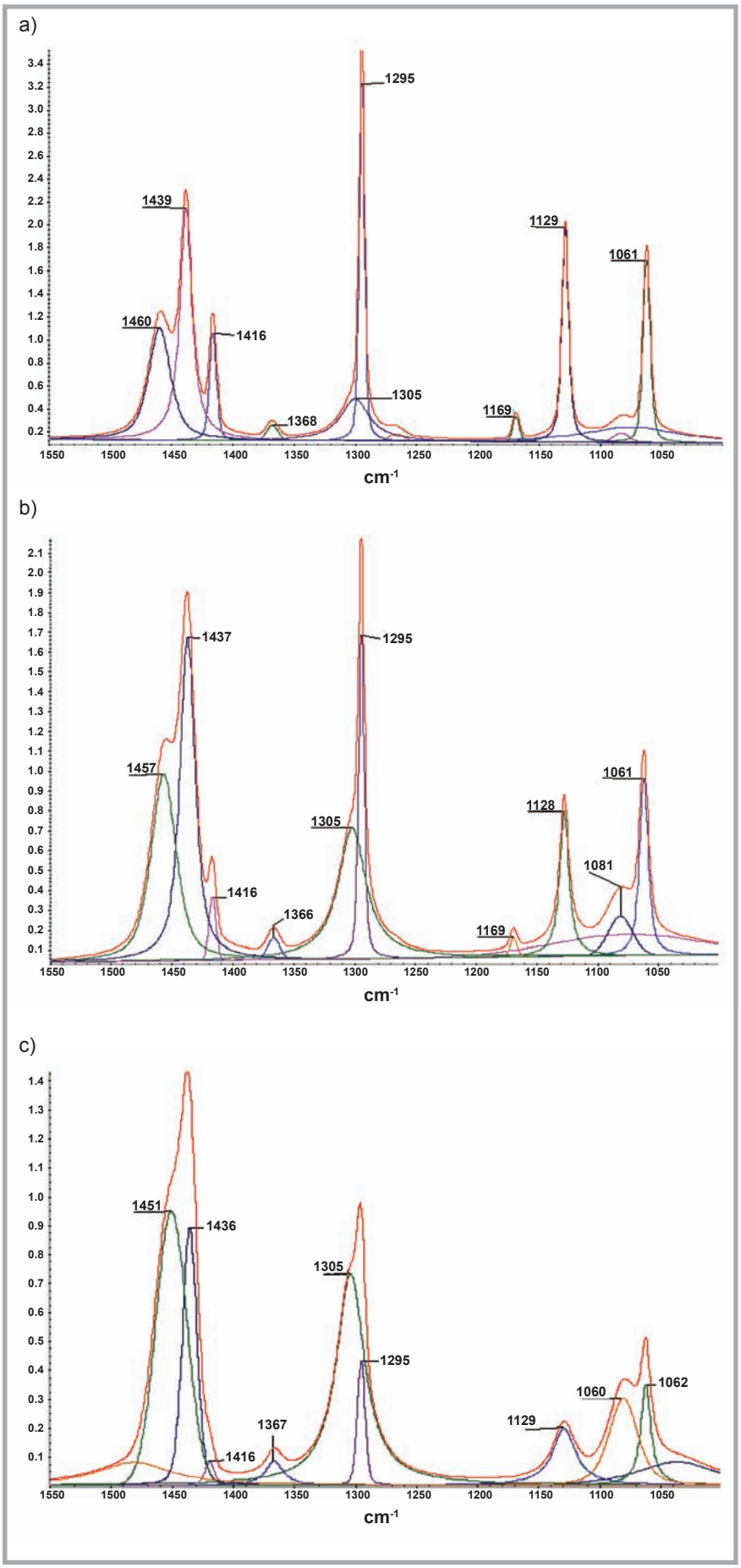

Figure 9. *Raman spectrum of the sample resolved into individual bands: a) EO1, b) EO5, c) EO8.*

Table 2. *Mass fractions of amorphous (A), crystalline (C) and transition (T) phases determined with WAXS and Raman methods.*

Sample	Mole % of 1-octene	CH_3/1000	WAXS			Raman		
			A_X	C_X	T_X	A_R	C_R	T_R
HDPE	+	+	32	53	15	31	65	4
LPE	0	0	33	55	12	31	68	1
EO1	0.8	3.9	43	48	9	43	48	9
EO2	1.77	8.4	56	37	7	54	31	15
EO3	4.34	19.2	66	31	3	66	14	20
EO4	5.42	23.3	67	30	3	68	17	15
EO5	5.5	23.6	69	28	3	70	13	17
EO6	6.64	27.7	70	28	2	69	13	18
EO7	9.15	35.9	88	10	2	90	5	5
EO8	11.27	42.1	92	8	-	91	2	7

$$C_R = \frac{I_{1416}}{0.46 \cdot I_{tw}} \qquad A_R = \frac{I_{1303}}{I_{tw}} \qquad (2)$$
$$T_R = 1 - (A_R + C_R)$$

where: I_{1416} and I_{1303} are the integral intensities of the bands located at 1416 cm^{-1} and 1303 cm^{-1}, I_{tw} is the integral intensity of the whole twisting vibrations region used as a standard and 0.46 is a scaling coefficient obtained for a completely crystalline polyethylene.

The Raman spectra were decomposed into individual bands using a least-squares curve fitting method implemented in the computer program GRAMMS, universally used in the analysis of infrared spectra. The bands were approximated by a linear combination of the Gauss and Lorentz functions. Three examples of Raman spectra for the EO1, EO5 and EO8 samples are shown in ***Figure 9.a-c*** (see page 61).

The results of the calculations are given in ***Table 2***. The comparison shows that the mass fractions of the transition and crystalline phases determined with the X-ray diffraction and Raman spectroscopic methods differ considerably. On the other hand, the mass fractions of the liquid–amorphous phase are very similar. The correlation between the results obtained for this parameter is shown in ***Figure 10***. It is evident that the "degrees of amorphicity" determined with the WAXS and Raman methods coincide very well with each other. In other words, the total mass fraction of the ordered and partially ordered phases is estimated similarly with the two methods; however, the individual fractions are different. Such discrepancies may be caused by the fact that the transition phase is "seen" differently in these two methods. Moreover, to calculate the mass fraction of the crystalline phase in the Raman method, we have to isolate the band 1416 cm^{-1} from a broad CH_2 bending range (1430-1550 cm^{-1}) composed of 4 bands. In the case of samples with medium and low crystallinity (see ***Figure 9***), such a decomposition may result in an underestimation of this band and as a consequence of too low a mass fraction of the crystalline phase and, in turn, too high a mass fraction of the transition phase (see Equation 2).

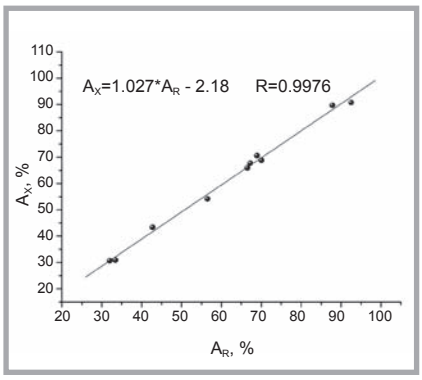

Figure 10. *Comparison of the mass fractions of the amorphous phase determined with the WAXS method (A_X) and with the Raman spectroscopic method (A_R).*

Conclusions

The existence of a third, transition phase that is intermediate in the degree of order between the crystalline and amorphous phases has already been proved in several papers dedicated to the structure of polyethylenes. In this work, we tried to determine how to account for the third component in the analysis of the WAXS diffraction curves of polyethylenes. It was shown that the best fit of the theoretical curves to the experimental data was obtained when the suggestions of Baker [11] were adopted. In this approach, two additional peaks representing the third phase are introduced. The additional peaks are located close to the crystalline reflections (110) and (200), on the left sides of these reflections. As a consequence, the third phase is treated as a quasi-orthorhombic one. Based on the angular positions of these peaks, found from the decomposition of the WAXS patterns, the density of the third phase was estimated. The obtained results show that, when the number of side branches in a polyethylene chain increases, the density smoothly decreases from the values close to the density of the crystalline phase, in the case of linear polyethylene, to the values close to the density of the amorphous phase, for the copolymers with high 1-octene content. The crystallinity and mass fraction of the transition phase also decrease continuously with increasing 1-octene content.

A comparison of the mass fractions of all three phases determined with the WAXS method and the Raman spectroscopic method shows that the total amounts of crystalline and transition phases estimated with these two methods agree very well. However, the values obtained for each individual phase do not coincide. The discrepancies may be caused by a different "perception" of the transition phase in these methods and by problems with the isolation of the "crystalline" band at 1416 cm^{-1} in the Raman spectra of the samples with high 1-octene content.

References

1. *McFaddin D., Russel K., Wu G., Heydig R.J. Polym. Sci. (1993), 31, 175.*
2. *Simanke A., Alamo R.G., Galland G., Mauler R.S. Macromolecules (2001), 34, 6959.*
3. *Sajkiewicz P., Hashimoto T., Saijo K., Gradys A. Polymer (2004), 46, 513.*
4. *Rabiej S. Fibres&Text. (2005), 5, 30.*
5. *Strobl R.G., Hagedorn W. J.Polym. Sci. Polym. Phys. Ed. (1978), 42, 1181.*
6. *Rabiej M., Rabiej S. "Analiza rentgenowskich krzywych dyfrakcyjnych polimerów za pomocą programu komputerowego WAXFIT", Publishing House ATH, Bielsko-Biała 2006.*
7. *Rabiej M. Polimery (2002), 47, 423.*
8. *Rabiej M. Fibres&Text. (2003), 5, 83.*
9. *Monar K., Habenschuss A. J. Polym. Sci. Polym. Phys. Ed. (1999), 37, 3401.*
10. *Bartczak Z., Gałęski A., Argon A.S., Cohen R.E. Polymer (1996), 37, 2113.*
11. *Baker A.M.E, Windle A.H., Polymer, 42, (2001), 667.*
12. *Swan P.R. J. Polym. Sci. (1960), 42, 525.*

Received 23.05.2008 Reviewed 21.11.2008